INFLUENCE OF Fe(III) IONS ON THE NICKEL HYDROXIDE ELECTRODE DURING LONG-TERM CYCLING

I. KREJČÍ* and J. MRHA

J. Heyrovský Institute of Physical Chemistry and Electrochemistry, Czechoslovak Academy of Sciences, 102 00 Prague 10 (Czechoslovakia)

B. FOLKESSON and R. LARSSON

Inorganic Chemistry 1, Chemical Center, University of Lund, P. O. Box 124, S-221 00 Lund (Sweden)

(Received October 27, 1986)

Summary

The iron-poisoning effect of sintered nickel oxide electrodes in alkaline accumulators during long-term cycling has been studied by electrochemical measurements, X-ray photoelectron spectroscopy and elemental analysis. Long-term cycling with periodic measurements of the discharge capacity, charge and discharge characteristics showed that both the quantity of iron and the way in which the iron is introduced play a large role in the poisoning.

Introduction

The iron-poisoning effect often occurs in alkaline Ni–Fe and, sometimes, even in Ni–Cd accumulators; it has already been described and studied by several authors [1 - 6], but there is no satisfactory explanation of the mechanism involved.

In Ni–Fe accumulators, almost all of the iron adsorbed on the positive electrode comes from the negative one, independent of whether it is of the pocket or the sintered type. In Ni–Cd accumulators the effect is smaller, but it can occur if iron is present in the active material of the cadmium electrode, and α-Fe_2O_3 is frequently added. Small amounts of iron may also originate from metallic construction elements, namely, current collectors, perforated steel strips (with pocket electrodes) and lugs, if they are not nickel-plated. The amount of iron thus transferred into the active material is small, but in some cases it is not negligible, *e.g.*, nickel oxide electrodes with a central current collector.

*Author to whom correspondence should be addressed.

0378-7753/87/$3.50

The solubility of $Fe(OH)_2$ or FeOOH in alkaline medium at normal temperature is low. If the iron electrode is polarized to the potential of oxygen evolution, however, it passes into the electrolyte as FeO_4^{2-} ions which decompose slowly to FeOOH and oxygen. Ferrate(VI) ions, according to our experience, are formed in the Ni–Fe cell during deep discharge, when the polarity of the electrodes is reversed and oxygen is evolved at the iron electrode, a rather rare case in practice.

Iron poisoning decreases both the conductivity of the nickel oxide, resulting in the formation of insulating barrier layers [1], and the oxygen overvoltage, resulting in a low charging efficiency [2, 3]. The more uniform the distribution of the FeOOH in the positive electrode, the greater is the effect.

The object of the present work was to study the effect iron has on the nickel hydroxide electrode and to correlate the electrochemical results with X-ray photoelectron spectroscopy (XPS) and with elemental analysis by atomic absorption spectroscopy (AAS).

Experimental

3 × 4.5 cm electrodes were cut from 0.75 mm thick commercial sintered nickel oxide electrodes. They were first formed with four cycles (16 h charging at 0.06 A, and a 0.1 A discharge to a cut-off potential of 0.0 V *versus* Hg/HgO in the same electrolyte). The reference electrode was separated from the KOH electrolyte (density, 1.2 g cm^{-3}) by a Haber–Luggin capillary. Thereafter the electrodes were subjected to long-term testing (details given below) either in a half-cell arrangement (with a nickel sheet as counter electrode) or in laboratory cells with an iron electrode (pocket or pressed type).

The capacity (C_s, mA h cm^{-2}) of the positive electrodes, some of which were doped with iron ions, was determined at the beginning of the measurements by discharging at 7.5 mA cm^{-2}. All subsequent discharges proceeded at the same current density with further treatment as below for the different electrodes:

Ni 1: Blank experiment, half-cell arrangement with a Ni sheet as a counter electrode.

Ni 2: Formed in a half-cell then cycled in a cell with a pocket Fe electrode.

Ni 3: Formed in a half-cell then cycled with a pressed Fe electrode.

Ni 4: Formed in a half-cell then washed in distilled water, dried, immersed for 1 min in a 20% solution of $Fe(NO_3)_3$, rinsed, immersed in 25% KOH, washed, dried, and cycled again in a half-cell arrangement.

Ni 5: As Ni 4, but immersed for 10 min in the solution of $Fe(NO_3)_3$.

Ni 6: As Ni 4 or Ni 5, but without immersion in the $Fe(NO_3)_3$ solution (blank experiment).

Accelerated cycling was carried out automatically and consisted of 40 min charging and 20 min discharging; the depth of discharge (DOD)

removed 60% of the experimentally available capacity, recharge input was 150%. Samples were cut from the electrodes at intervals (after every measuring cycle for the determination of the discharge capacity) for XPS measurements. Charge/discharge (E–t) curves were recorded during every measuring cycle and during accelerated cycling, with special note being made of the end potential (charging or discharging).

For the XPS measurements 6 X 13 mm samples were cut from the electrodes then washed and dried. An overall spectrum was first recorded for every sample and then the areas of interest, *i.e.*, Ni $2p_{3/2}$, Fe $2p_{3/2}$, O_{1s} and C_{1s}.

The measured kinetic energy E_{kin} is related to the inner core electron binding energy, E_b, by the relation

$$h\nu = E_{kin} + E_b + \varphi$$

where $h\nu$ = 1486.6 eV and is a correction term [7, 8]. In the presentation of the results, E_{kin} of Fe, Ni and O have been corrected to the same E_{kin} of C_{1s}. This value was chosen to correspond to $E_b(C_{1s})$ = 285.0 eV.

The elemental analysis was made by dissolving a piece of the electrode in 12 M HCl and measuring the concentration of Ni and Fe by atomic absorption spectroscopy (AAS). From these data the bulk concentrations of Fe and Ni in the oxide layer could be calculated.

The XPS method on the other hand gives the concentrations of the elements on the surface of the oxide layer.

TABLE 1

Weight percent. of Fe and Ni found in the oxide gel layer by AAS and XPS

Sample	Elemental analysis AAS			XPS
	Ni (%)	Fe (%)	$\frac{Fe}{Ni} \times 100$	$\frac{Fe}{Ni} \times 100$
3/1	64.0	0	0	0
3/2	62.6	1.2	1.9	9
3/3	63.4	0.60	0.9	19
3/4	63.4	0.55	0.8	23
4/1	61.9	2.2	3.6	7
4/2	59.9	4.0	6.7	2
4/3	61.4	2.6	4.2	0
4/4	60.0	4.0	6.7	0
5/1	61.2	2.8	4.6	15
5/2	61.1	2.8	4.6	14
5/3	61.5	2.5	4.1	11
5/4	56.0	7.9	14.1	0

The error limits of the elemental analysis by AAS are about 1% (Ni) and 5% (Fe). The error limits of the estimated Fe/Ni-values by XPS are about 10%.

Absolute concentrations cannot, however, be easily measured, but one can calculate the relative concentrations. By measuring the areas of the peaks, and using previously determined sensitivity factors for Ni and Fe respectively, the ratio Fe/Ni in the surface can be obtained. Such sensitivity factors vary from one type of instrument to another and must be determined experimentally.

From the integrated area of $2p_{3/2}$ peaks using well-defined samples we obtained a sensitivity factor for Fe of 2.4 and for Ni of 4.1, both related to that of C_{1s}. In the last column of Table 1 we present the Fe/Ni ratio of various electrode samples. Care has to be taken in measuring the peak area as irreproducable broadening may be caused by charging of the sample.

Results and discussion

Cycling performance of the positive electrode under iron-free conditions

Our initial measurements were devoted to comparing the behaviour of nickel oxide electrodes with different counter-electrodes. The results are shown graphically in Fig. 1 (electrodes Ni 1 - 3), where the capacity per unit area, C_s, is plotted against the number of accelerated cycles. With a nickel sheet as a counter electrode (electrode Ni 1), the value of C_s decreased after 125 cycles as was expected for systems without Li^+ or Co^{2+} additives, [*cf.* refs. 9 - 11]. This sudden decrease in the capacity of electrode Ni 1 can be understood from the XPS data obtained using some samples taken from the electrode. Figures 2 and 3 give some representative spectral details. The initial Ni $2p_{3/2}$ spectra exhibit one major peak and a "satellite" peak which are clearly resolved. As the electrochemical operations proceed, however, one notes that the Ni spectra become more blurred and less well

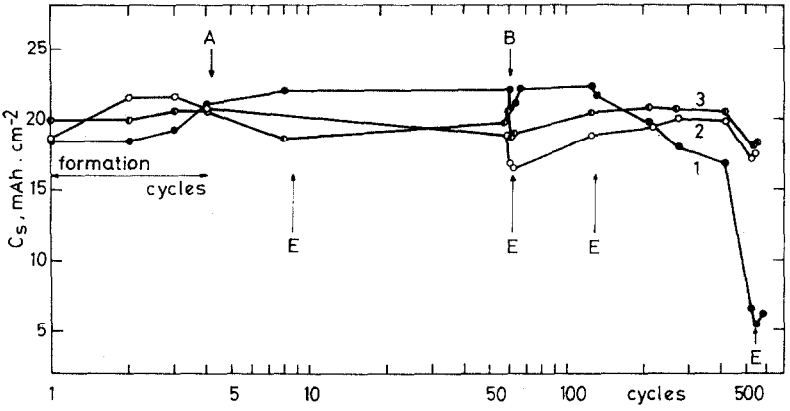

Fig. 1. Influence of different counter-electrodes on the specific capacity, C_s, of the nickel oxide electrode. 1, Nickel sheet counter-electrode; 2, pocket iron counter-electrode; 3, pressed iron counter-electrode; E, electrolyte exchange; A, addition of different counter electrodes; B, removal of pocket iron counter-electrode.

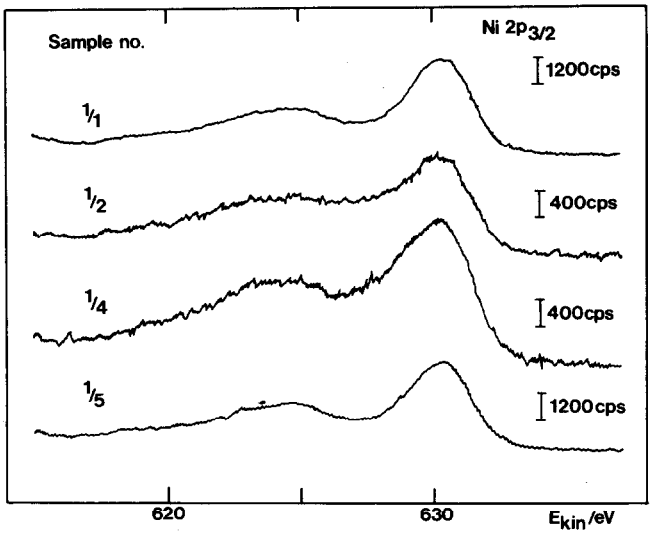

Fig. 2. XPS spectra of Ni $2p_{3/2}$ core electrons of electrode Ni 1.
Sample 1/1 was taken after 4 cycles
1/2 after 61
1/4 after 528
1/5 after 566.
For technical reasons, samples 1/2 and 1/4 were much smaller in size than the others.

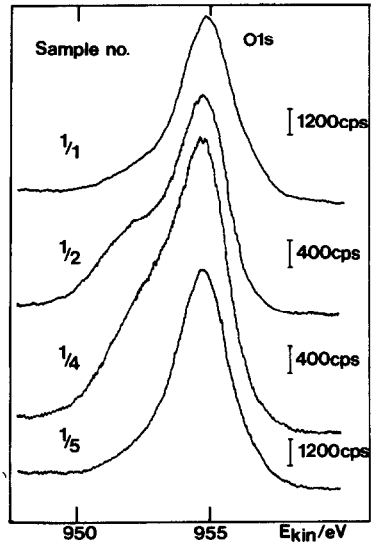

Fig. 3. XPS spectra of O_{1s} core electrons of Ni 1 electrode. Sample numbers are the same as given in Fig. 2.

resolved. At the same time one observes additional components of the O_{1s} peaks at low kinetic energy, indicating charging of the specimen by the loss of electrons. Such charging will reduce the resolution of the Ni spectrum. It originates from the low electrical conductivity of the sample and a fully conducting specimen does not exhibit charging. Furthermore, it may be observed that the last spectrum of the series (Figs. 2, 3) shows a renewed sharpness and the absence of the O_{1s} peaks. From this we suggest the following: at the start the semiconducting $NiOOH/Ni(OH)_2$ layer is in good mechanical and electrical contact with the nickel backing (support). During the electrochemical charging/discharging this $Ni(OH)_2/NiOOH$ system is exposed to shrinking/expansion cycles when the system behaves like a hydrogel with variable molar volume [12, 13]. During cycling, this gel gradually loses its mechanical and electrical contact with the nickel support, at least at some spots, which creates the necessary conditions for uneven charging. After a number of cycles this decreasing mechanical contact between oxide gel layer and the Ni-support results in the dispersion of the oxide into the electrolyte.

The XPS spectra now have sharp peaks again, revealing the existence of a new nickel oxide phase formed on the surface of the nickel backing during long term cycling. This new oxide phase is in good contact with the support. The dispersion of material into the electrolyte, however, results in a sudden decrease in the capacity of the electrode as there is now less active material. A similar explanation holds for the Ni 6 electrode.

Influence of an iron counter electrode on the positive electrode

With a pressed-type iron counter-electrode a decrease in the capacity of the Ni 3 electrode took place after 410 cycles; cycling was ended after 560 cycles for technical reasons.

The capacity per unit area of the Ni 2 electrode, when coupled with a pocket iron electrode, decreased slowly during 61 accelerated cycles (Fig. 1). Thereafter, the negative electrode failed and was replaced by a nickel sheet. On further cycling, the original capacity of the Ni 2 electrode was restored and did not decrease further until the end of cycling. The characteristics of the positive electrodes combined with iron electrodes have only slightly lower values of C_s ("weak" iron-poisoning effect), as can be seen from Fig. 1.

The iron electrode also seems to have some stabilizing effect on the capacity of the positive electrode, as the break in the capacity *versus* time curve occurs later for the Ni 2 and Ni 3 electrodes than for Ni 1.

The favourable influence of the iron electrode was further manifested in the discharge characteristics (at the 3 h rate), as can be seen from Fig. 4 where curves 1 and 2 refer to positive electrodes with nickel, and curves 3 and 4 to those with pressed iron counter electrodes. The discharge curves are given after 65 (curves 1 and 3) and 412 accelerated cycles (2 and 4). The favourable effect of the pressed iron electrode is apparent from the shift of the discharge curves to more positive potentials.

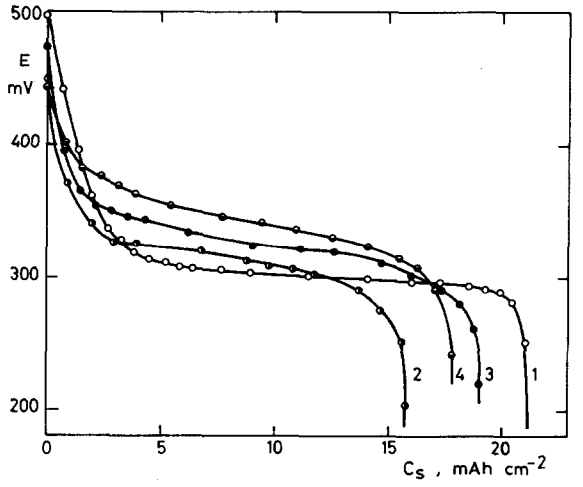

Fig. 4. Typical discharge curves of nickel oxide electrodes combined with two different counter-electrodes. 1, Nickel sheet counter-electrode, cycle 65; 2, nickel sheet counter-electrode, cycle 412; 3, iron counter-electrode, cycle 65; 4, iron counter-electrode, cycle 412.

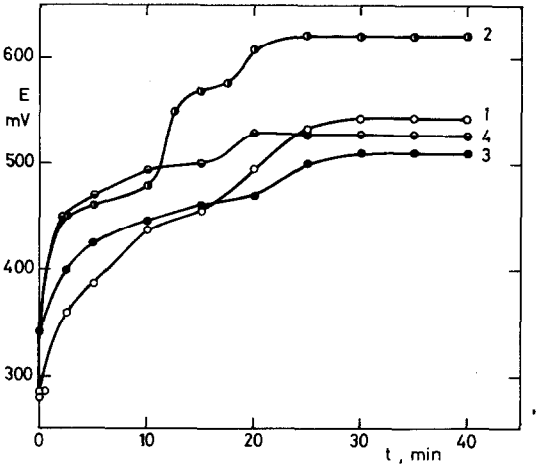

Fig. 5. Typical charging curves of nickel oxide electrodes combined with two different counter-electrodes (10 min = 5 mA h cm^{-2}). 1, Nickel sheet counter-electrode, cycle 53; 2, nickel sheet counter-electrode, cycle 410; 3, iron counter-electrode, cycle 54; 4, iron counter-electrode, cycle 410.

The charging curves of the positive electrodes (at a 0.7 h rate) are shown in Fig. 5 after 53 and 54 (curves 1 and 3) and 410 accelerated cycles (2 and 4). Curves 1 and 2 refer to Ni 1 electrode (with a Ni counter electrode), and 3 and 4 to electrode Ni 3 (with a pressed iron electrode). It can be seen that the Ni 1 electrode has a higher oxygen overpotential which

increases with the number of accelerated cycles, whereas the Ni 3 electrode has a lower oxygen overpotential which does not increase during cycling.

During the "effective" period of charging (*i.e.*, the initial stage), after 54 or 410 accelerated cycles the working potential of the positive electrode is shifted to more positive values in the presence of the iron electrode than in its absence. A similar potential shift is caused by long-term cycling.

On the whole, the charging characteristics of the positive electrode are flatter with, than without, the iron electrode. The presence of iron probably causes parasitic evolution of oxygen on the positive electrode during the first stage of charging (Figs. 5 and 9). As a result, the electrode cannot be fully charged, *i.e.*, its capacity is lowered. Replacement of the iron electrode with the nickel counter electrode causes a gradual weakening of the effect of iron, although some stabilizing effect on the discharge still remains.

The iron content of electrodes Ni 2 and Ni 3 was determined after 4, 61, 125 and 528 accelerated cycles.

The XPS and AAS results for the Ni 3 electrode are summarised in Table 1. This electrode was studied more thoroughly because unlike electrode Ni 2 it had been cycled under unchanged conditions during the whole test.

One can see that the Fe/Ni ratio is much higher in the surface layer than in the bulk material. Furthermore, there is a continuous increase of iron at the surface as cycling proceeds, see Fig. 6 and Table 1. (Note that when interpreting the Fe spectra of Fig. 6 one should use the total peak areas.) There is, however, no corresponding increase of bulk concentration. Rather, it seems from Table 1 that the iron to nickel ratio decreased somewhat after having reached an initial peak value. It can be seen that this

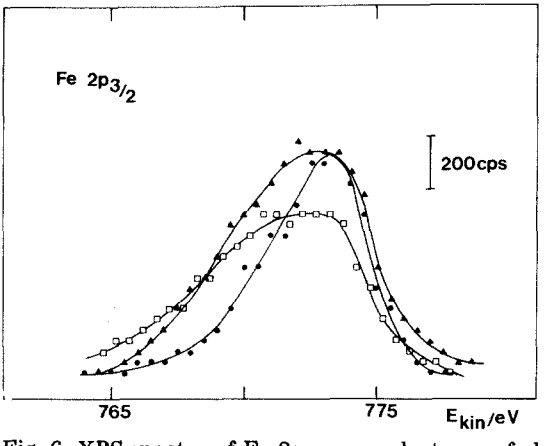

Fig. 6. XPS spectra of Fe $2p_{3/2}$ core electrons of electrode Ni 3.
●, sample taken after 61 cycles;
▲, sample taken after 125 cycles;
□, sample taken after 528 cycles.
Note the increased broadening of the peaks resulting from increased surface charging (*cf.* the text).

decline in the bulk concentration of iron is accompanied by a partial restoration of the discharge capacity of the positive electrode (see Fig. 1).

Treatment of the positive electrode with a solution of Fe(III) ions

Electrodes Ni 4 - 6 were used to investigate the effect of doping the nickel oxide electrode with Fe(III) ions. The results of accelerated cycling of these electrodes are shown in Fig. 7, where the values of C_s are plotted against the number of cycles. It can be seen that the treatment with $Fe(NO_3)_3$ caused a significant decrease in the capacity after only the 8th cycle: with the Ni 4 electrode to 73% and with Ni 5 to 58% of the original value, whereas the capacity of the Ni 6 electrode (as with the Ni 1 - 3 electrodes) was unaltered, as expected up to the 125th cycle. The decrease in the capacities of the Ni 4 and 5 electrodes is much larger than with Ni 2 and 3 and is related to the duration of immersion in the iron nitrate solution. During long-term cycling the iron poisoning of the Ni 4 electrode gradually grew weaker, its original capacity being restored after 125 cycles. The other electrode, however, did not recover fully, which was doubtless due to the prolonged treatment with the iron nitrate solution.

On further cycling (125 - 560 cycles) the capacity of the Ni 4 electrode decreased in a manner similar to that of Ni 1 or Ni 6, whereas in the case of Ni 5 a gradual restoration of the capacity took place, followed by a decrease after 400 cycles (Fig. 7).

It follows from the above findings that the "weak" iron poisoning effect (Ni 2 and 3 electrodes), caused by the presence of the iron electrode, is manifested by a certain stabilization of the discharge capacity during long-term cycling. The "strong" iron-poisoning effect (Ni 4 and 5 electrodes), on the other hand, induced by treatment of the nickel oxide electrode with $Fe(NO_3)_3$, causes a decrease in the discharge capacity.

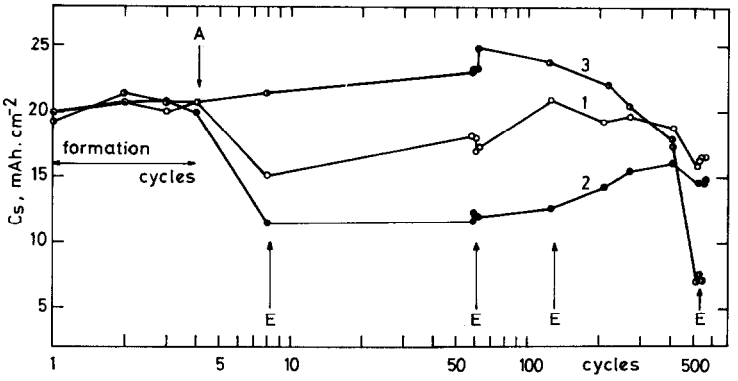

Fig. 7. Influence of different treatments by iron ions on the specific capacity, C_s, of the nickel oxide electrode. 1, Short immersion of the nickel oxide electrode in solution of Fe(III) ions (Ni 4); 2, long immersion of the nickel oxide electrode in solution of Fe(III) ions (Ni 5); 3, blank experiment (Ni 6); A, addition of Fe(III) ions; E, electrolyte exchange.

A comparison of the discharge characteristics of the electrodes with and without doping with Fe(III), after various numbers of accelerated cycles (Fig. 8), reveals that the initial working potential of the Fe-doped electrode (Ni 5) is higher than that of the undoped (Ni 6) electrode. The difference is even more marked after 125 cycles when the discharge potential of the doped electrode is practically unchanged, whereas that of the undoped electrode is markedly shifted to less positive values. These results can be compared with the similar effect of "weak" iron poisoning shown in Fig. 4. Thus, both the strong and the weak Fe-poisoning is favourable for the discharge potential of the nickel oxide electrode, especially after many accelerated cycles.

The charging characteristics of the Fe-doped (Ni 5) and undoped (Ni 6) electrodes are shown in Fig. 9. The characteristics of the latter are in good agreement with those for the Ni 1 electrode (Fig. 5) and is evidence for the reproducibility of the electrode preparation. The characteristics of the Ni 5 electrode are, after 54 cycles, still flatter than for Ni 3 (Fig. 5), since the evolution of oxygen proceeds at the end of the charging period at +470 mV for Ni 5 and at +510 mV for Ni 3. The decreased oxygen overpotential causes the decrease in the capacity of the electrode treated with $Fe(NO_3)_3$.

To compare electrodes with one another we introduced a criterion for the charging capability of the nickel oxide electrode: the difference between the potential after 40 min charging (the last portion of the charging curve) E_{40} and after 15 min charging (the end of the "effective" portion of the charging curve), E_{15}, *i.e.*, $\Delta E = E_{40} - E_{15}$. This reflects the difference between the oxidation potential of $Ni(OH)_2$ and the potential of oxygen evolution. The higher the value of ΔE, the higher is the charge acceptance of the

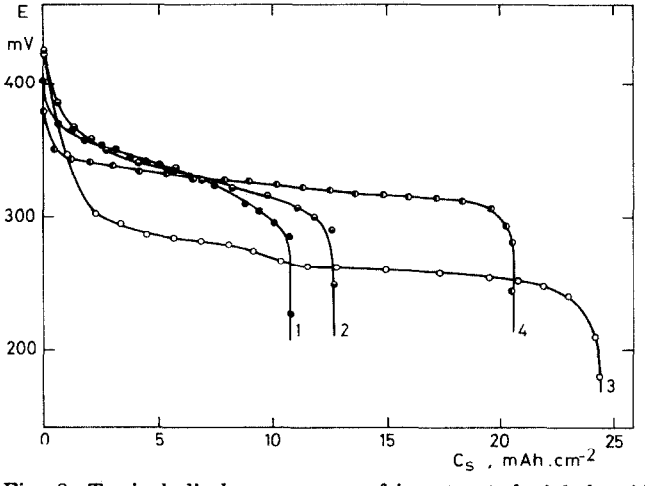

Fig. 8. Typical discharge curves of iron-treated nickel oxide electrodes. 1, Fe(III) treatment, cycle 8; 2, Fe(III) treatment, cycle 125; 3, without treatment, cycle 125; 4, without treatment, cycle 4.

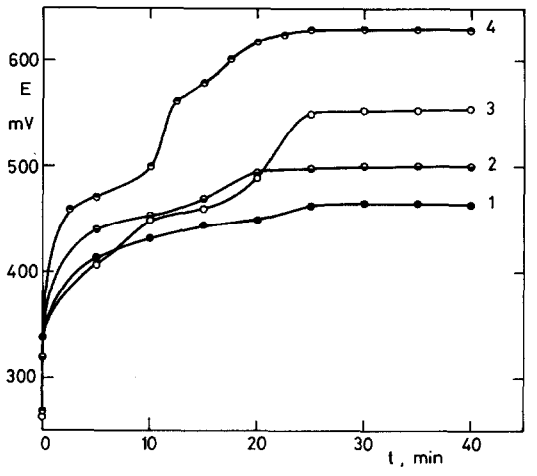

Fig. 9. Comparison of untreated and Fe(III) treated nickel oxide electrodes (10 min = 5 mA h cm^{-2}). 1, Fe(III) treatment, cycle 54; 2, Fe(III) treatment, cycle 411; 3, without treatment, cycle 54; 4, without treatment, cycle 411.

electrode. Selected values of ΔE are given in Table 2, where it is seen that the "standard" nickel oxide electrodes Ni 1 and Ni 6 have a relatively high charge acceptance after 53 accelerated cycles, hence a high discharge capacity also.

The Ni 3 electrode showing a "weak" Fe-poisoning effect has a lower ΔE value than the Ni 1 and Ni 6 electrodes. Electrode Ni 5, with "strong" Fe-poisoning, has the minimum value of ΔE. After 410 accelerated cycles the values of ΔE for the Ni 1 and Ni 6 electrodes dropped to one half, similar to their discharge capacity and charge acceptance, as did Ni 3. Electrode Ni 5, however, shows no change in the ΔE value and, accordingly, no change in the low charge acceptance during the whole cycling test. Thus, the stronger Fe-poisoning effect is manifested after 53 cycles by a lower charge acceptance and, hence, by a drop in the discharge capacity. In a later stage of the cycling test (after 410 cycles), the charge acceptance of all electrodes

TABLE 2

Electrode no.	E (mV)		Fe-poisoning effect
	Number of cycles		
	53	410	
Ni 1	110	50	no
Ni 6	100	50	no
Ni 3	60	30	"weak"
Ni 5	25	25	"strong"

decreased, the decrease being only slight for the electrode with the strongest Fe-poisoning effect.

The XPS and AAS results for the Ni 4 and Ni 5 electrodes present interesting differences compared with those of Ni 3. As an example, Fig. 10 shows some XPS spectra of the Ni 5 electrode. There is a peak which must correspond to metallic nickel. This means that one can see some parts of the nickel support. This metallic nickel, however, only appears in spectrum 5/3 after 125 cycles. The spectrum representative of the first cycling periods (5/2) shows very little difference from that of electrode (5/1), tested immediately after the iron treatment.

From the data of Table 1 we conclude that:

the bulk concentrations of iron in electrodes Ni 4 and Ni 5 are much higher than was the case for electrode Ni 3;

the surface concentration of iron on the other hand, decreases markedly with the number of electrochemical cycles (*cf.*, Figs. 11, 12). This decrease is accompanied by a restoration of electrode capacity (Fig. 7).

As the iron content of the bulk is high it seems logical that the nickel oxide gel is severely influenced by the iron salt treatment. It is not possible to decide whether the adverse electrochemical effect (strong Fe-poisoning) is caused by this chemical attack of the nickel hydroxide, $NiOOH/Ni(OH)_2$, system or of the backing nickel support. In view of the high acidity of a strong $Fe(NO_3)_3$ solution, perhaps both effects operate.

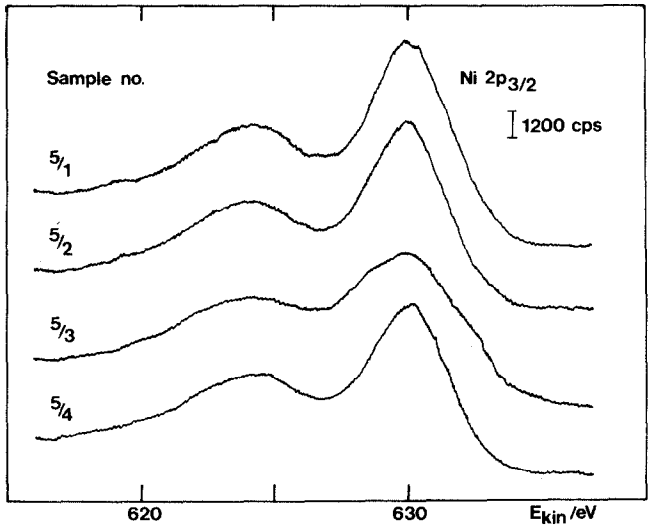

Fig. 10. XPS spectra of Ni $2p_{3/2}$ core electrons of electrode Ni 5. Sample 5/1 was taken after 4 cycles; sample 5/2 after 61, sample 5/3 after 125 and sample 5/4 after 528 cycles.

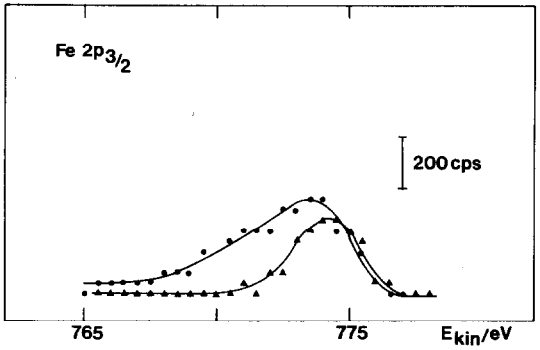

Fig. 11. XPS spectra of Fe $2p_{3/2}$ core electrons of electrode Ni 4.
●, sample taken after 4 cycles;
▲, sample taken after 61 cycles.

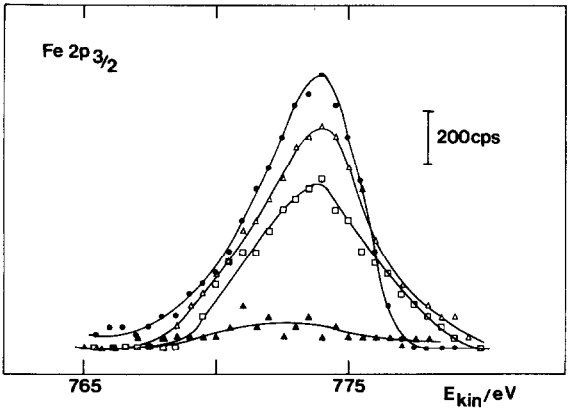

Fig. 12. XPS spectra of Fe $2p_{3/2}$ core electrons of electrode Ni 5.
●, sample taken after 4 cycles;
△, sample after 61;
□, sample after 125;
▲, sample after 528 cycles.

Conclusions

If a sintered nickel oxide electrode (undoped with Li and Co) is combined with an iron electrode, it shows only a moderate decrease in the discharge capacity ("weak" Fe-poisoning effect). It is also relatively stable during long-term cycling, and its discharge potential is shifted to more positive values. It seems that, in a manner similar to that of cobalt hydroxides, traces of iron hydroxides have a beneficial effect on the structure or conductivity of the active material.

By contrast, the treatment of the electrode with a strong acidic $Fe(NO_3)_3$ solution causes a strong Fe-poisoning effect, *i.e.*, a considerable drop in the charge acceptance and thus, also in the discharge capacity. This overcompensates the beneficial effect of traces of Fe transferred from the iron electrode to the positive electrode.

From the spectroscopic observations it seems likely that the decline in capacity of positive electrodes working under iron-free conditions is caused by gradual destruction of the original $NiOOH/Ni(OH)_2$ gel. It seems that this destruction is counteracted by the presence of iron, evenly distributed in the bulk of the oxide gel.

Acknowledgements

This work was financially supported by the Swedish Board for Technical Development (STU). The ESCA instrument was bought from a grant by the Bank of Sweden Tercentenary Fund. The visit to Lund by I. Krejčí was part of an exchange programme between the Czechoslovak Academy of Sciences and the Swedish Academy of Engineering Sciences.

The technical assistance of Mrs Sylvia Flato in the atomic absorption spectroscopic measurements is also gratefully acknowledged.

References

1 R. Z. Tichenor, *Ind. Eng. Chem.*, *44* (1952) 973.
2 D. Tuomi, *J. Electrochem. Soc.*, *112* (1965) 1.
3 G. Troilius and G. Alfelt, in D. H. Collins (ed.), *Power Sources, Pergamon Press*, Oxford, 1967, p. 337.
4 S. U. Falk and A. J. Salkind, *Alkaline Storage Batteries*, Wiley, New York, 1969, p. 631.
5 G. Mlynarek, M. Paszkiewicz and A. Radniecka, *J. Appl. Electrochem.*, *14* (1984) 145 - 149.
6 M. Z. A. Munshi, A. C. C. Tseung and J. Parker, *J. Appl. Electrochem.*, *15* (1985) 711.
7 K. Siegbahn, C. Nordling, A. Fahlmann, R. Nordberg, K. Hamrin, J. Hedman, G. Johansson, T. Bergmark, S. E. Karlsson, I. Lindgren and B. Lindberg, *ESCA–Atomic, Molecular and Solid State Structure Studied by Means of Electron Spectroscopy*, Almqvist and Wiksell, Uppsala, 1967.
8 B. Folkesson and R. Larsson, *Chem. Scr.*, *10* (1976) 105.
9 P. Oliva, J. Leonardi, J. F. Laurent, C. Delmas, J. J. Braconnier, M. Figlarz, F. Fievet and A. de Guibert, *J. Power Sources*, *8* (1982) 229.
10 R. Barnard, C. F. Randell and F. L. Tye, *J. Appl. Electrochem.*, *11* (1981) 517.
11 R. D. Armstrong, G. V. D. Briggs and M. A. Moore, *Electrochim. Acta*, *31* (1986) 25.
12 K. Micka, J. Mrha and B. Klápště, *J. Power Sources*, *5* (1980) 207 - 214.
13 J. Jindra, I. Krejčí, J. Mrha, B. Folkesson, L. Y. Johansson and R. Larsson, *J. Power Sources*, *13* (1984) 123 - 136.